Laser-induced incandescence and elastic-scattering measurements of particulate-matter volume fraction changes during passage through a dilution tunnel

by

Robert M. Green and Peter O. Witze
Combustion Research Facility
Sandia National Laboratories
Livermore, CA 94551, USA

Published in the *Proceedings of the 10th International Symposium on Applications of Laser Techniques to Fluid Mechanics*, Lisbon, July 2000

ABSTRACT

Modern diesel engines produce far less mass of particulate matter than their predecessors, but this advance has been achieved at the expense of a significant increase in the number of sub-micron sized particles. This change in soot morphology has created the need for new instrumentation capable of measuring small volumes and sizes of particulate matter in a reasonable period of time, and preferably in real-time. Laser-induced incandescence and laser elastic scattering are complementary techniques suitable for this task. Optical measurements are presented for a diesel engine exhaust and compared with measurements performed using a scanning mobility particle sizer. This study investigates the effects of exhaust dilution and temperature control of the sampling system. It is also shown that laser-induced vaporization of low temperature volatile material is a potentially valuable technique for measuring the volatile component of exhaust particulate matter.

1. INTRODUCTION

The U.S. Environmental Protection Agency (EPA) has established both the particulate matter (PM) regulations and the measurement procedures to be used to certify compliance of diesel vehicles. The EPA procedure specifies the use of exhaust dilution which is intended to replicate the dilution of exhaust as it occurs in typical applications to produce PM as it is found in the atmosphere. It is also essential that the amount of dilution is sufficient to prevent water condensation at 52 °C, the maximum temperature specified for the filter paper that is used to collect the sample. However, because there are no set guidelines for line lengths, line temperatures and residence time following dilution, the amount of volatile organic matter adsorbed by the soot particles during their passage to the filter paper can vary significantly, altering both the volume fraction and size of the particles impinging on the filter. While this does not affect the mass of PM collected with the gravimetric procedure (as a first approximation, most volatiles, with the exception of water, are collected by the filter paper), it will alter the size distribution and volume fraction measured with a scanning mobility particle sizer (SMPS). Because diesel PM size and number are now recognized to have a significant effect on health risks, it is imperative to understand the size-change effects due to volatile organic matter adsorption, as well as other phenomena, during the residence time following dilution.

Laser-induced incandescence (LII) is a powerful optical diagnostic for the study of PM because it can be applied in any environment encountered as the exhaust gas travels from the combustion chamber to the atmosphere, and has been estimated to be sensitive to concentrations as low as one part per trillion (Wainner et al., 1999). Schraml et al. (1999) have demonstrated the use of LII in raw diesel exhaust, and Snelling et al. (2000) have reported measurements for diluted diesel exhaust. LII involves the use of a high-energy laser beam to heat carbon particles to their vaporization temperature. Thermal emission, i.e., incandescence, from the particles is then recorded and used to estimate the particle volume fraction and primary particle size. The LII technique is inherently simple when the following assumptions apply: 1) Soot particles are small compared to the laser wavelength (Rayleigh regime); 2) Laser heating increases the temperature of all particles at the same rate, regardless of size; 3) When the particles reach the vaporization temperature, additional absorbed energy goes into vaporization rather than sensible energy, so that once they reach the vaporization temperature, all particles remain at the same temperature for the duration of the laser heating period; 4) Finally, vaporization causes negligible particle-size reduction, so that the incandescent radiation

from the particles is independent of laser fluence F when $F>F^*$, the fluence at which significant vaporization begins. This "plateau" feature of the LII signal is extremely useful for its practical application, because it allows quantitative measurements without concern for the absolute value of laser fluence, as long as F^* is exceeded. This is particularly important for applications where laser beam extinction is non-negligible, such as two-dimensional imaging of soot-laden flames. Corrections for extinction are unnecessary if the laser fluence exceeds F^* by more than the losses from extinction.

The assumption regarding the existence of a plateau region, where LII is independent of laser fluence, is the most precarious of those just listed. In general, a plateau does not occur because laser-induced vaporization (LIV) of soot results in measurable mass loss (Dasch, 1984). Because LII is proportional to particle volume, a seemingly small 10% loss in diameter represents a 27% reduction in LII signal level. The fact that the plateau has been observed in practice is purely fortuitous, and is a direct result of a nonuniform spatial profile of the laser beam. Ni et al. (1995) and Tait and Greenhalgh (1993) have shown that a plateau can be achieved with a Gaussian laser profile, for which the effective probe volume (based on the dynamic range of detectivity) increases with increased fluence to compensate for mass loss from vaporization along the beam centerline. In contrast, a top-hat laser beam profile can lead to an LII signal that drops significantly as laser fluence is increased beyond F^* (Ni et al., 1995). Although Vander Wal and Jensen (1998) have shown that normalized LII signals obtained at difference fluences exhibit self-similar behavior, they also conclude that quantitative measurements require calibration at a specified laser fluence.

In addition to LII, laser elastic scattering (LES) will occur and lead to both beneficial and detrimental consequences. The negative aspect is that LES from the PM under investigation as well as the walls and windows of the LII optical cell can reduce the signal-to-noise characteristics of the LII measurement. This situation can be significantly improved by optical filtering, or totally avoided by gated detection of the LII signal after the end of the laser pulse. The beneficial role of LES is that it can complement the LII. Whereas LII involves radiative emission from light-absorbing particles (essentially limited to solid carbon), LES responds to both solid and liquid phase PM. The liquid phase PM includes the soluble organic fraction (SOF, principally organic material derived from fuel and lubricating oil) and sulfate particulates (hydrated sulfuric acid). In addition, LES in the Rayleigh regime is proportional to $N_p D_p^6$, where N_p is the number of primary particles and D_p is the primary particle diameter, while LII is proportional to $N_p D_p^3$. Thus it is technically possible to ratio these two quantities to obtain a measure of the primary particle number and size; unfortunately, in the context of vehicle emissions, the number of agglomerated particles and their size are far more important quantities. (The primary particle size does provide insight into the surface area of particulates (Snelling et al., 2000), which has health issue ramifications.) However, in terms of PM composition, i.e., solid carbon versus SOF, the combination of LII, LES, and LIV may prove to be a useful diagnostic tool, and is the main subject of this paper.

2. ENGINE & EXHAUST-SAMPLING SYSTEM

As a source of diesel engine exhaust for the experimental measurements reported in this work, we used a 1996 Volkswagen, 1.9L TDI diesel engine. The important characteristics of this engine are listed in Table 1.

Table 1
1996 1.9L Volkswagen TDI Engine

Engine Type	4 Cylinder Turbo DI
Injection System	Pump, line, nozzle
Displacement	1896 cm^3
Bore	79.5 mm
Stroke	95.5 mm
Compression Ratio	19.5:1
Rated Output	66 kW @ 4000 rpm
Maximum Torque	202 Nm @ 1900 rpm
Emission Control	Intercooled EGR

The engine, which was removed from a car following about 50,000 miles of operation, was mounted on a test stand in the laboratory. A compact, water-brake dynamometer was used for power absorption, and a closed-loop coolant system was employed to maintain proper coolant temperature. The stock Engine Control Module was used for primary engine-control management in the laboratory. However, we established auxiliary control capabilities with a laboratory PC for the accelerator position, the EGR

control valve and the water-brake, to allow external control of certain engine functions. The engine-control software allowed control of the speed, load and EGR flow for both steady-state as well as transient engine operation.

The exhaust sampling and dilution configuration is illustrated schematically in Fig. 1. The engine exhaust was sampled approximately 0.3 m downstream of the muffler using a pair of tubes having entrances oriented upstream to the flow direction. One of the tubes provided a flow of exhaust gas through sample lines heated to 100 °C to an ejector-pump diluter (manufactured by Dekati Ltd.) where the sample was diluted with dry nitrogen. Early in our work we determined that if the diluent and diluter were not heated, liquid condensation in the sample-line orifice located at the throat of the venturi in the diluter could seriously affect the operation of the diluter. Following the work of Maricq et. al. (1999), we found that heating the diluent and diluter to approximately 120 °C resolved that problem. For the experiments involving a diluted sample, we operated the diluter at a nominal dilution ratio of 10. When performing measurements on undiluted samples, we removed the sample-line orifice and turned off the flow of diluent. Upon exiting the diluter, the sample passed into both the optical cell where the LII and LES measurements were carried out, and the SMPS where the PM characteristics were also measured.

The second tube provided a flow of exhaust gas through a heated line to an electronic condenser where water vapor was removed from the sample flow. The dry exhaust gas was then directed to a non-dispersive, infrared (NDIR) gas analyzer where the CO_2 concentration was measured. In order to determine the dilution ratio, a pair of three-way valves allowed us to extract a fraction of diluted exhaust from below the diluter and redirect it to the condenser and NDIR analyzer, where the CO_2 concentration of the diluted exhaust was measured.

3. OPTICAL DIAGNOSTICS SETUP

The majority of LII/LES measurements reported in the literature have been obtained using gated detection of either

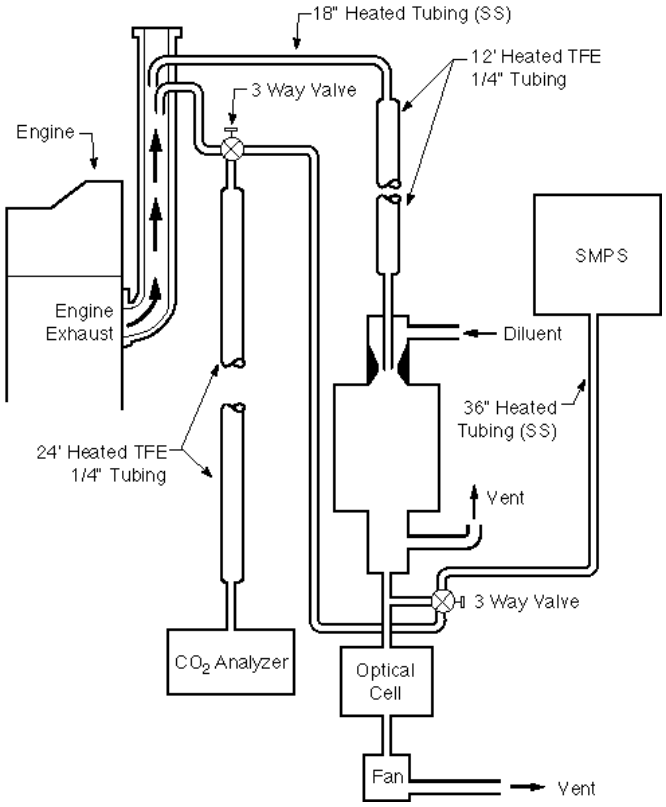

Figure 1. *Schematic diagram of the exhaust-sampling system illustrating the engine, ejector-type diluter, optical cell, and the SMPS. Also shown are the heated sample lines connecting the various components.*

electronic or optical (i.e., imaging) signals, and thus are time-averaged over the gate width. Our approach is to use a fast transient recorder to simultaneously acquire the electronic signals from multiple photodetectors, which allows us to use instantaneous values or mimic the response of a gated detector by integrating the signals. Our transient recorder has a 500 MHz bandwidth, and can digitize four channels simultaneously at 5 Giga-samples/sec. A GPIB interface allows complete computer control of the recorder. The temporal resolution of each LII/LES event is limited by the sampling rate of the digitizer. For the data to be presented, the acquisition rate was 10 GS/s, resulting in a 0.1 ns resolution, which was achieved by an analytic interpolation of the maximum digitization rate. Relative to the engine exhaust-flow time scale, the PM measurement temporal resolution is limited by the 10 Hz repetition rate of the laser.

A schematic of the experimental setup is shown in Fig. 2. The second harmonic (532 nm) output of a Nd:YAG laser was used for excitation; the maximum energy per pulse was 100 mJ. The spatial beam-profile was approximately Gaussian, and the beam was recolumated to a diameter of about 3 mm. The laser fluence was controlled using a half wave plate (HWP) and thin film polarizer (TFP). Three measurements were simultaneously obtained with fast photodetectors: 1) Incident temporal profile of the laser pulse, detected from diffuse scattering through a neutral density filter (NDF); 2) LII signal, detected through a long-wave pass filter with a 570 nm cutoff; 3) LES, detected through an NDF and an interference bandpass filter (BPF) centered at 532 nm, with a 10 nm full-width at half-maximum (FWHM). The laser pulse profile was used to determine the laser energy, and was calibrated using a slow-response, calorimeter-type power meter for a time-averaging period of 50 seconds.

Fast photodiodes (PD) with a rise time of 0.5 ns were used to detect the laser pulse and LES signals, but since the LII signal was much weaker, particularly with dilution, it was necessary to use a photomultiplier tube (PMT) for the LII. The tube selected had a rise time of 0.8 ns, an electron transit time of 7.8 ns, and a spectral response range of 300-650 nm. The PMT response was not linear over the full range of the LII signals, so we calibrated the response using incandescence from a laser-heated wire and a discrete set of neutral density filters.

4. SMPS RESULTS

The SMPS is generally considered the industry standard for measuring exhaust PM size distributions (Lemaire, 1998). It is a refined technology and, in principle, is straightforward to use. In practice, however, numerous problems arise in engine exhaust applications where the sample handling and conditioning is extremely important and

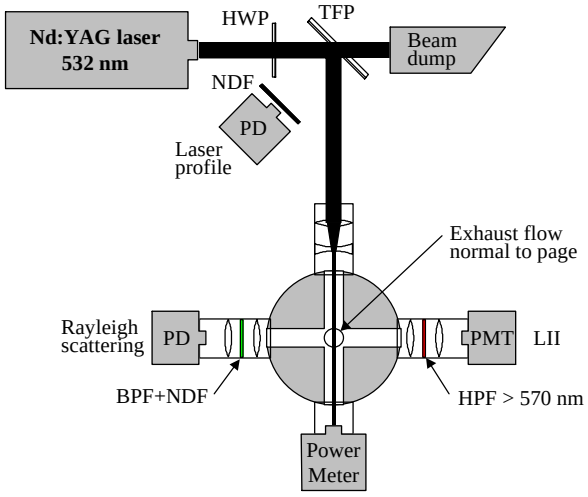

***Figure** 2. Schematic diagram of the layout of the optical diagnostic.*

can have a significant effect on measurements. In general, exhaust dilution is necessary to prevent overloading the particle counter in the SMPS; in addition, vapor condensation within the SMPS may disrupt the sample-flow control and could interfere with the internal operation of the instrument, leading to invalid measurements. In the current work, we operated both with and without dilution in order to determine the sample-handling limits for use of the SMPS in diesel engine exhaust applications. Furthermore, we examined the effects of heating the diluent and the body of the diluter

Initially, we operated the sampling system with the 1m by 6.4 mm diameter line between the diluter and the SMPS inlet at room temperature. However, we observed that the SMPS data would be steady only for a short time before an increase in large particle sizes would begin; concurrently, the critical flow rate into the SMPS would begin to drift. We attributed this behavior to condensation of water in this sample line or even within the SMPS itself, and decided to heat the sample line to greater than 100°C. Furthermore, when diluting the exhaust sample with the diluter housing and the diluent at room temperature, we observed that the dilution ratio slowly, but continuously, increased. An examination of the sample orifice/nozzle in the diluter revealed the presence of water, which was impeding the flow of exhaust gas, leading to an increase in the dilution ratio. Based on this observation, we installed a capability to heat the diluent gas and the body of the diluter to a temperature greater than 120 °C. This alteration of the diluter setup resulted in complete elimination of the slow variation of the dilution ratio. In addition, heating the diluter housing also eliminated the accumulated condensed water that we observed on the impacter at the entrance of the SMPS when operating without dilution and with the diluter body cold.

The experience described above has left us with some very serious concerns regarding handling of exhaust samples from diesel engines, similar to the observations of Kittleson and Johnson (1991). First, and probably most significant, is the fact that when operating undiluted with a cold diluter housing, the SMPS data are seriously suspect due to condensation problems. Second, if the diluent and diluter housing are cold when operating diluted, problems maintaining a steady dilution ratio cast doubt on the resulting SMPS data. Third, when operating undiluted with the diluter housing hot, we observed that the results from the SMPS were neither consistent nor steady. Finally, when the sample is diluted with heated diluent and the diluter housing is heated, we observed the best conditions for reliable SMPS data. In spite of these problems, we still chose to report SMPS data for all four test conditions. Because we were aware of the indicators of potential problems, we feel that the results, while not precise for the colder conditions, are “representative” from a comparative viewpoint.

Summarized in Fig. 3 are the particle size distribution measurements, where the SMPS dynamic range was set for

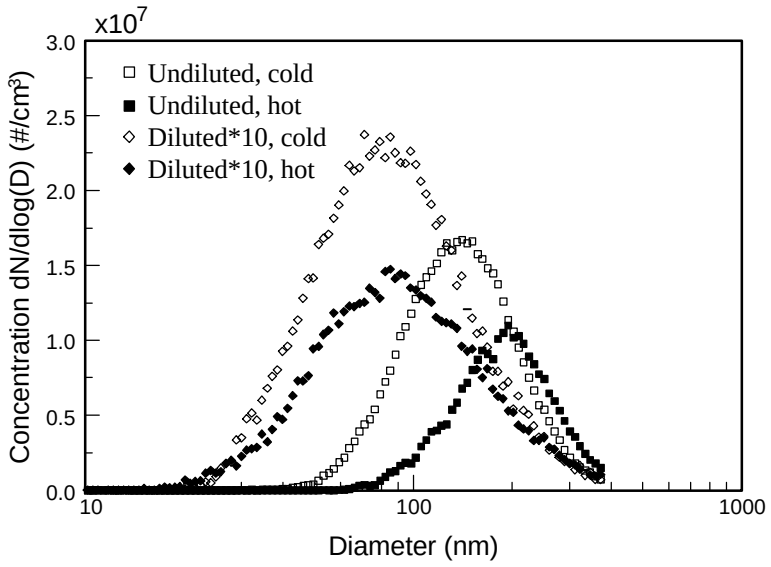

Figure 3. *Particle size distributions for the four dilution/temperature conditions.*

10-380 nm. The results for the diluted samples have been multiplied by ten for direct comparison with the measurements for undiluted samples. The size distributions for hot and cold, diluted, are similar, but there are more particles for the cold condition, which may be due to increased nucleation of sulfates following dilution (Abdul-Khalek et al., 1998). For the undiluted conditions, the size distributions are very different, and unexpected in that the hot case is characterized by fewer, but larger particles within the distribution. We can only speculate as to the cause of this situation, but it may be that when the body of the diluter is heated when there is no dilution, nucleation of new particles is inhibited to a greater degree than the growth of the existing particles.

Presented in Fig. 4a is the cumulative, particle volume fraction, where again the diluted measurements have been multiplied by ten. The impact of the very large particles for the undiluted, hot case are clearly evident. Because particles smaller than 100 nm do not contribute measurably to the total volume fraction, the LII measurements, which depend on particle volume, are expected to be preferentially sensitive to the larger particles.

The particle size distributions presented in Fig. 3 suggest that the Rayleigh criteria (particle size much less than the laser wavelength) is reasonably satisfied, so it can be assumed that the intensity of the LES, I_{LES}, is proportional to FD^6. Therefore, $\sqrt{I_{LES}/F}$ is also an approximate measure of the particle volume fraction, but is also even more biased by large particles than LII. Fig. 4b shows the cumulative sixth-power of the SMPS particle size measurements. These results illustrate the heavy weighting of the LES signal by large particles - those particles less than 200 nm are essentially insignificant.

5. LII & LES RESULTS

Typical LII and LES temporal profiles for several different laser fluences are presented in Fig. 5. The 50 ns record length was resolved to 0.1 ns, and the data were averaged for 400 laser shots. The LES data show the expected monotonic increase in intensity with laser fluence; however, these results are not directly proportional because there is background interference from wall flare that has not been accounted for in this figure. The dip in the LES signals near the maximum is caused by higher output modes of the unseeded Nd:YAG laser. The delay between the maxima of the LES and LII signals is due to the electron transit time of the PMT. This is more clearly illustrated by the bold-dotted LES curve that was recorded by the PMT. This curve also reveals the poorer response time of the PMT compared to the PD (0.8 versus 0.5 ns, respectively), and the effect of transit-time spread. Because the LII signal can be

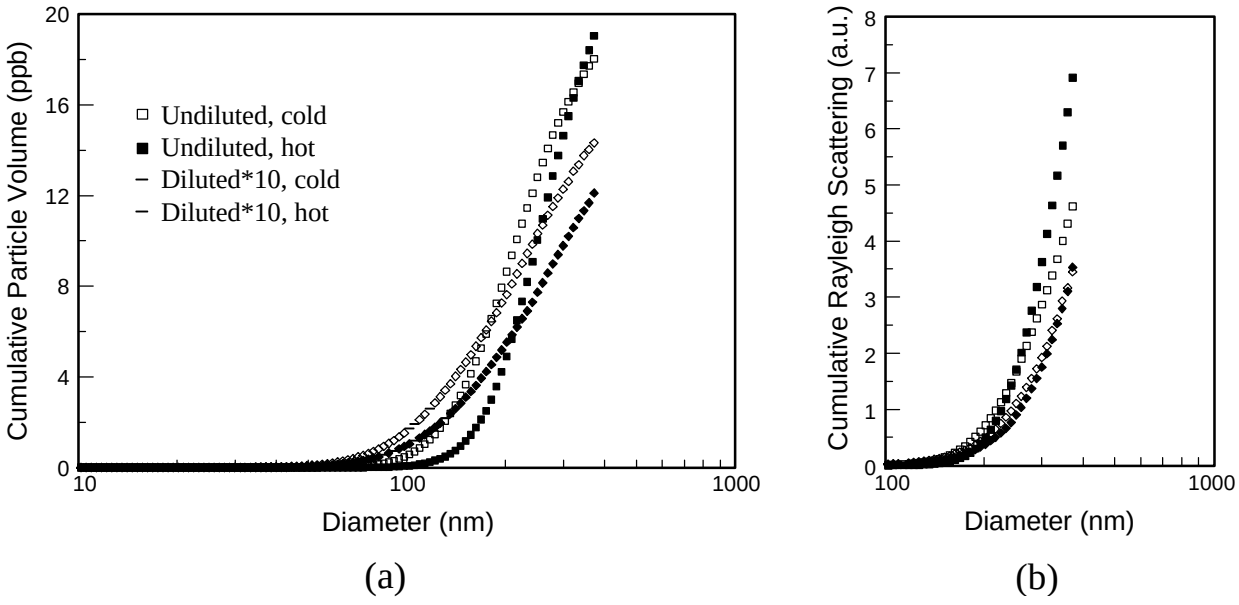

Figure 4. ***a.)*** *Cumulative particle volume concentration for the four dilution/temperature conditions illustrating how LII is sensitive to larger particles;* ***b.)*** *Cumulative particle diameter to the sixth power illustrating how LES is even more sensitive to larger particles.*

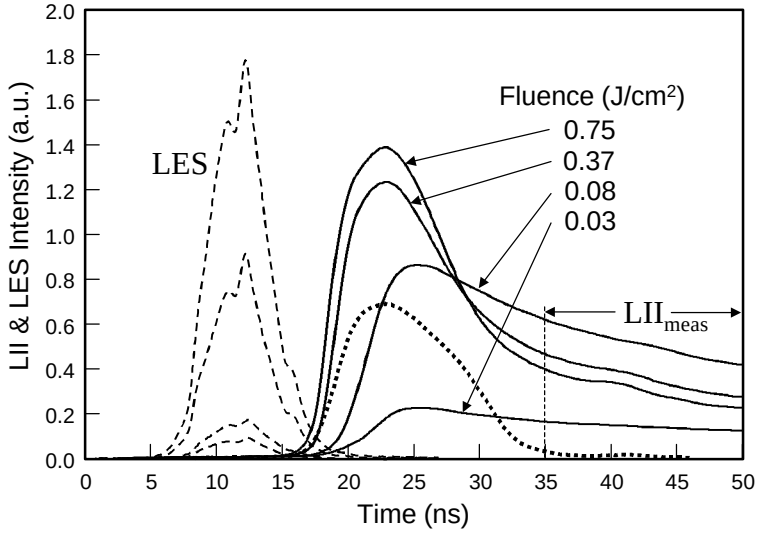

Figure 5. *Temporal profiles of LII (solid) and LES (dashed) signals. The heavy dotted curve is LES data obtained with the PMT, illustrating the difference in temporal response between the PD and the PMT.*

quite weak, it is sensitive to background interference from both LES and laser-induced fluorescence (LIF). In order to minimize these problems, we calculate the LII magnitude as the area under the LII signal from 35 to 50 ns. Similarly, the LES magnitude is calculated as the area under the LES signal from 0 to 25 ns. We also subtract background interferences measured with the optical cell purged with nitrogen.

The LII measurements are summarized in Fig. 6a as a function of laser fluence. Note that we have multiplied the diluted measurements by the dilution ratio of 10, so the results shown are a direct comparison of the exhaust volume fractions. For the undiluted/cold case, the LII reaches a nearly constant-value plateau for fluences greater than F^*

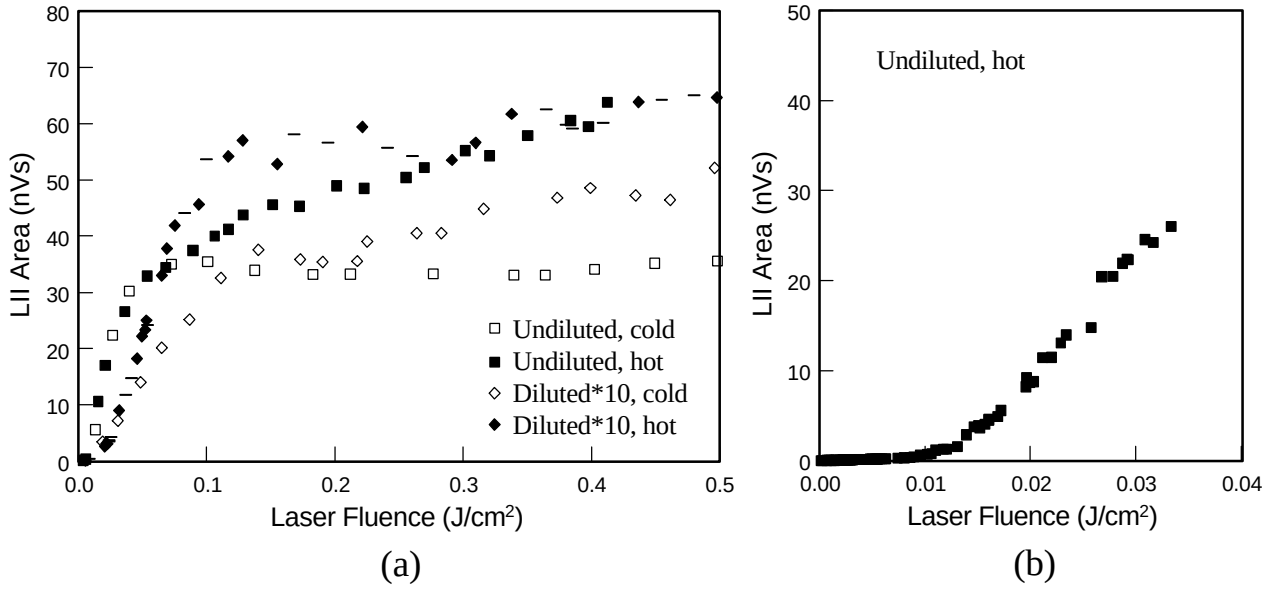

Figure 6. a.) *LII signals as a function of laser fluence for the four dilution/temperature conditions;* ***b.)*** *Expanded low-fluence region for the undiluted/hot case.*

(where mass loss from vaporization becomes measurable). On the other hand, for the three other cases, following F^* the LII is characterized not by a constant-value plateau, but by a continuous increase in signal. As mentioned earlier, the possibility of the LII being independent of laser fluence for $F>F^*$ is a consequence of the spatial profile of the laser beam, which in this case is approximately Gaussian. As the fluence is increased, solid carbon is vaporized near the centerline of the laser profile at the same time as low-temperature SOF is vaporized farther out in the Gaussian wings. Because LII is proportional to temperature as T^5 (in the Rayleigh regime, the inverse wavelength dependence of the emissivity adds an additional power of T beyond the typical T^4 dependence), the wings do not contribute significantly to the signal until the temperature approaches the vaporization point of carbon (>4000 K), long after the SOF has vaporized. A major consequence of SOF condensed on solid carbon is the endothermic effect of the vaporization process prior to significant heating of the carbon; condensed volatiles containing no carbon are not expected to contribute to the LII signal. We expect that without dilution, there is significantly more condensation of volatile material on the carbon particles than when dilution is used. Thus, the particles in the Gaussian wings are at lower temperatures for the undiluted cases because more heat has gone into vaporization of SOF.

Detailed interpretation of the results presented in Fig. 6a is complicated by the fact that absorption by carbon particles is dramatically altered in the presence of large amounts of weakly absorbing substances. Bohren and Huffman (1983) estimate that a 1% by volume suspension of carbon within a nonabsorbing sphere will absorb about 3 times more energy than carbon in just air. Fuller et al. (1999) estimate a similar enhancement-factor. The increase is due to two effects, an increase in absorption cross section and a focusing of the incident light onto the carbon particle.

Presented in Fig. 6b are LII measurements for the undiluted/hot case at very low fluences. They are included to illustrate the behavior of the signal during the early heating period. The slow rate of increase of LII for fluences less than 0.01 J/cm^2 perhaps indicates that much of the laser energy is going into vaporization of SOF rather than temperature rise of solid carbon.

As mentioned earlier, we can estimate the relative PM volume fraction using the square root of the magnitude of the LES signal divided by the fluence. These results are summarized in Fig. 7a as a function of laser fluence; this estimate assumes that the number of primary particles N_p does not change with fluence. Note that we have again multiplied the diluted measurements by the dilution ratio. It is important to recall that the LES signals are integrated over the entire laser-pulse duration, and thus the result represents a complex convolution of the temporal variation of particle size and laser energy. Early in the laser pulse, the laser intensity is low, but the PM is at its largest size, particularly if heavily laden with condensed water and SOF; later, as the laser intensity increases the volatiles vaporize,

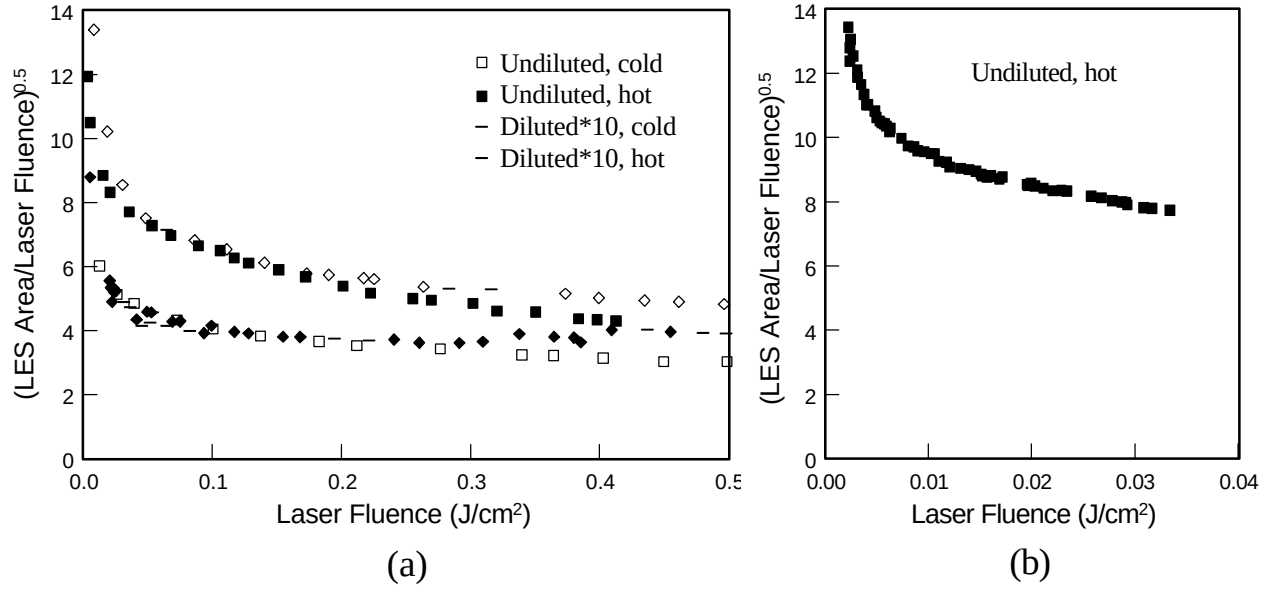

Figure 7. a.) *Processed LES signals (relative volume fraction) as a function of laser fluence for the four dilution-temperature conditions;* ***b.)*** *Expanded low-fluence region for the undiluted/hot case.*

reducing particle size. At high laser fluences, vaporization of the volatiles will occur very early in the laser pulse, and thus will not contribute to the LES. However, even at the low laser intensities in the wings of the Gaussian beam profile, the D^6 dependence of LES (for the Rayleigh regime) may result in measurable contribution to the total LES signal.

For all four test conditions at the low fluence levels, the LES is seen to fall very rapidly with increasing fluence. Based on the observed value of F^*, we can estimate that the carbon particle temperatures reach ~4000 K when the fluence is of the order of 0.1 J/cm^2. So we can expect a significant loss in particle volume at much lower fluences must be due to vaporization of condensed volatiles. The magnitude of the LES for the undiluted/cold case is very surprising, in that we would expect it to be the largest, when in fact it is very similar to the diluted/hot results, which we expect should be, and is, the smallest. The SMPS results presented in Fig. 4b do show the cumulative Rayleigh scattering signal for undiluted/cold to be considerably less than for undiluted/hot, but not as low as the diluted cases.

Similar to the previously-discussed effect of condensed volatiles on the absorptivity of carbon particles, scattering cross sections are also altered. Michelsen (2000) has estimated that PM that is 40% SOF by volume (a reasonable upper-limit for diesel exhaust), with the carbon randomly positioned within droplets, will have an effective scattering cross section that is only 60% that of pure carbon. Thus, we can expect that the measurements in Fig. 7a for the undiluted and cold cases may be low because of a reduced cross section, and thus do not accurately represent the volume fraction of PM.

In Fig. 7b we show detailed measurements made at very low fluences; the limited dynamic range of the photodetectors prevented us from resolving a region of constant volume where the liquid phase is being heated, prior to the onset of vaporization. Indeed, it is very difficult to make measurements of this type at very low fluences, where the relative error in the measured fluence can become significant, such that division by the fluence can have dramatic effects.

6. SUMMARY & CONCLUSIONS

Figure 8a summarizes the particle volume fractions measured by the LII, LES and SMPS techniques, normalized by the respective fraction for the diluted/hot case. The optical measurements are for a laser fluence of 0.15 J/cm^2. Shown in Fig. 8b are the corresponding SMPS mean particle diameters weighted by number and volume, which can be helpful in interpreting the volume fraction measurements. In general, several general conclusions can be made: 1.) The SMPS results are mostly as expected, with increased volume fraction for the conditions most likely to include condensates. The detailed differences for the undiluted cases may be unimportant, because the SMPS is not

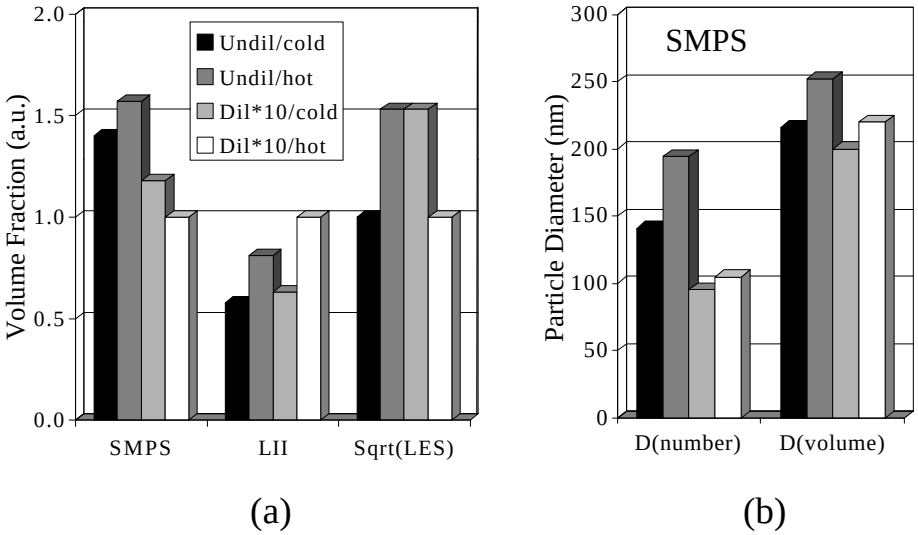

Figure 8. a.) *Comparison of particle volume fraction measurements by SMPS, LII and LES;* ***b.)*** *Mean particle diameters, number and volume weighted, measured with the SMPS.*

well suited for these conditions; 2.) The LES results are reasonably similar to the SMPS data, which we would expect since they both respond to condensed volatiles and carbon; 3.) The LII results are considerably different from the other two measurements, which is expected because of the signal sensitivity to carbon only. The highest values occur for the diluted/hot case, suggesting that energy consumption by the vaporization of volatile material is significant. However, the competing effects of particle size and absorption and scattering cross sections makes data interpretation difficult.

Perhaps the most significant observation of this study is the strong dependence of the LII, LES and SMPS measurements to condensed PM. We believe that fundamental investigations of two-phase aerosols (carbon plus a single-component liquid) will lead to a better understanding of LII and LES signals in the presence of LIV, and the eventual development of a useful diagnostic for the measurement of the volatile and solid carbon volume fractions in engine exhaust. The major advantage of the optical techniques over particle sampling is the former can, in principle, be applied everywhere from the engine cylinder to the atmosphere. In practice, there is a large amount of work that needs to be done before quantitative optical measurements will be possible.

ACKNOWLEDGEMENT

This work was performed at the Combustion Research Facility of the Sandia National Laboratories, and was funded by the U.S. Department of Energy, Office of Transportation Technologies. The authors are grateful for technical assistance from Hope Michelsen and Dale Tree of Sandia in preparation of the manuscript, and the help of Greg Smallwood and Dave Snelling of the National Research Council of Canada with identification of the cause of a data anomaly. Finally, we wish to thank the DOE Office of Basic Energy Sciences for providing us with the diluter and SMPS.

REFERENCES

Abdul-Khalek, I. S., Kittleson, D. B. and Brear, F. (1998). "Diesel Trap Performance: Particle Size Measurements and Trends," SAE Paper No. 982599.

Bohren, C. F. and Huffman, D. R. (1983). Absorption and Scattering of Light by Small Particles, John Wiley & Sons, Inc., pp. 443-446.

Dasch, C. J. (1984). "Continuous-Wave Probe Laser Investigation of Laser Vaporization of Small Soot Particles in a Flame," *Applied Optics* 23, No. 13, pp. 2209-2215.

Fuller, K. A., Malm, W. C. and Kreidenweis, S. M. (1999). "Effects of Mixing on Extinction by Carbonaceous Particles," *J. Geophys. Res.* 104, No. D13, pp. 15,941-15,954.

Kittleson, D. B. and Johnson, J. H. (1991). "Variability in Particle Emission Measurements in the Heavy Duty Transient Test," SAE Paper No. 910738.

Michelsen, H. A. (2000). Private communication, Sandia National Laboratories.

Lemaire, J. (1998). "World's Scientists Aim to Define Critical Ultrafine PM Issues," *Diesel Fuel News*, September 21.

Ni, T., Pinson, J. A. Gupta, S. and Santoro, R. J. (1995). "Two-Dimensional Imaging of Soot Volume Fraction by the Use of Laser-Induced Incandescence," *Applied Optics* 34, No. 30, pp. 7083-7091.

Schraml, S., Will, S. and Leipertz, A. (1999). "Simultaneous Measurement of Soot Mass Concentration and Primary Particle Size in the Exhaust of a DI Engine by Time-Resolved Laser-Induced Incandescence (TIRE-LII)," SAE Paper No. 1999-01-0146.

Snelling, D. R., Smallwood, G. J., Sawchuk, R. A., Neill, W. S., Gareau, D., Clavel, D. J., Chippior, W. L., Liu, F., Gülder, Ö. L. and Bachalo, W. D. (2000). "In-Situ Real-Time Characterization of Particulate Emissions from a Diesel Engine Exhaust by Laser-Induced Incandescence," SAE Paper No. 2000-01-1994.

Tait, N. P. and Greenhalgh, D. A. (1993). "PLIF Imaging of Fuel Fraction in Practical Devices and LII Imaging of Soot," *Phys. Chem.* 97, No. 12, pp. 1619-1625.

Vander Wal, R. L. and Jensen, K. A. (1998). "Laser-Induced Incandescence: Excitation Intensity," *Applied Optics* 37, No. 9, pp. 1607-1616.

Wainner, R. T., Seitzman, J. M. and Martin, S. R. (1999). "Soot Measurements in a Simulated Engine Exhaust using Laser-Induced Incandescence," *AIAA J.* 37, No. 6, pp. 738-743.